Langmuir Article

pubs.acs.org/Langmuir


# On the Possible Role of Surface Elasticity in Emulsion Stability

Daniela Georgieva,[†] Véronique Schmitt,[‡] Fernando Leal-Calderon,[§] and Dominique Langevin*,[†]

[†]*Laboratoire de Physique des Solides, Université Paris Sud 11, 91400 Orsay Cedex, France,* [‡]*Centre de Recherche Paul Pascal, Université Bordeaux 1, CNRS UPR 8641, Avenue Schweitzer, 33600 Pessac, France and* [§]*TREFLE, Université Bordeaux 1, CNRS UMR 8508, Avenue des Facultés, 33405 Talence, France*

*Received December 23, 2008. Revised Manuscript Received February 17, 2009*

We have measured the short-time and long-time elastic responses to compression of various types of surfactant layers adsorbed at oil−water interfaces. We prepared reasonably monodisperse oil-in-water emulsions with the same surfactants and monitored the time evolution of the emulsion droplets' diameter. We used a broad variety of surfactants (cationic, nonionic, and small polymers) and alkanes with different chain lengths. The emulsion drop size evolution is first controlled by Ostwald ripening and later on by drop coalescence, the later step being quite short. The overall emulsion lifetime is therefore dominated by ripening and for a given oil appears well correlated with the low-frequency surface elasticity as expected (and not with the high-frequency one, which is expected to control coalescence). When the oil chain length is changed, the stability is related more to the oil solubility in water, which also controls ripening. The overall results demonstrate the great importance of surface elasticity in emulsion stability.

## I. Introduction

Emulsions are metastable dispersions made of two immiscible liquids, with one being dispersed into the other with the help of surface-active agents.[1,2] They are currently obtained by shearing the two fluids and incorporating one phase into the other. Emulsions are of considerable industrial importance in a broad range of applications such as cosmetics, foods, paints, and pharmaceuticals. Their stability depends on many parameters: drop size and polydispersity, drop volume fraction, solubility of the phase dispersed into the continuous one, and the presence of additives in the dispersed phase when they are insoluble in the continuous phase (for instance, salt in water or long-chain oils in short-chain oils). In addition, the stability also depends on the nature of the surface-active agents. Whereas the influence of the first parameters is reasonably well understood, the role of the surface-active agents remains unclear. It has been postulated that the important parameter affecting emulsion stability is surface rheology, but so far no clear picture has emerged. In this article, we will address this question using emulsions stabilized by surfactants, which are the simplest kind of surface-active agents.

Surfactant molecules adsorb spontaneously at the oil/water interface, thereby reducing the interfacial tension. A surfactant molecular layer forms at the oil−water interface. This layer is able to resist compression deformation and exhibits viscoelastic properties (elasticity and viscosity). It is possible to determine the dynamic compression (or dilatation) interfacial properties at air/liquid and liquid/liquid interfaces using different methods: oscillating bubbles/drops, oscillating barriers and Langmuir troughs, capillary wave propagation, surface light scattering, and others.[3] The layers can also resist shear, but for surfactants, the shear elastic modulus is zero (the layers are liquid) and the shear viscosity is much smaller than the dilatational viscosity. The shear viscoelasticity is therefore expected to play a small role.

The lifetime of emulsions may vary from a few minutes to many years, depending on the surfactant. Emulsion destruction occurs under the influence of several processes: sedimentation or creaming, Ostwald ripening (transfer of liquid from the smaller droplets to the larger ones by diffusion through the continuous phase driven by the difference in the Laplace pressure[4]), and coalescence (fusion of two droplets after rupture of the liquid film between them through the formation of a thermally activated hole[5,6]). The last process is similar to the rupture of isolated films on frames, and it is currently admitted that it is controlled by surface viscoelasticity. Ostwald ripening is mainly controlled by the solubility of the phase dispersed into the continuous one and by the dispersed-phase volume fraction. However, recent work suggested that the surface elasticity also plays an important role in this process.[7]

Little is yet known about the actual values of oil/water interfacial viscoelasticity of surfactant monolayers.[8−10] A huge difficulty is posed by the existence of surfactant exchange between the surface and bulk that lowers the surface viscoelastic parameters to a large extent, especially when the

*Corresponding author. E-mail: langevin@lps.u-psud.fr.

(1) Becher, P. *Encyclopedia of Emulsion Technology*; Marcel Dekker: New York, **1985**

(2) Leal-Calderon, F.; Schmitt, V.; Bibette, J. *Emulsion Science: Basic Principles*; 2nd ed.; Springer: New York, **2007**

(3) Langevin, D. In *Encyclopedia of Surface and Colloid Science*; Hubbard, A., Ed.; Marcel Dekker: New York, **2002** and references therein.

(4) Lifshitz, I. M.; Slyozov, V. V. *Sov. Phys. JETP* **1959**, *35*, 331.

(5) Langevin, D. *Adv. Colloid Interface Sci.* **2000**, *88*, 209 and references therein.

(6) De Gennes, P. G. *Chem. Eng. Sci.* **2001**, *56*, 5449.

(7) Meinders, M. B. J.; van Vliet, T. *Adv. Colloid Interface Sci.* **2004**, *108*, 119.

(8) (a) Lemaire, C.; Langevin, D. *Colloids Surf.* **1992**, *65*, 101. (b) Bonfillon, A.; Langevin, D. *Langmuir* **1993**, *9*, 2172. (c) Bonfillon, A.; Langevin, D. *Langmuir* **1994**, *10*, 2965. (d) Bonfillon, A.; Langevin, D. Unpublished observations. Ritacco, H.; Langevin, D. In preparation.

(9) Kim, J-H; Koczo, K.; Wasan, T. *J. Colloid Interface Sci.* **1997**, *187*, 29. Xu, W.; Nikolov, A.; Wasan, D.; Gonsalves, A.; Borwankar, R. *Colloids Surf., A* **2003**, *214*, 13.

(10) Santini, E.; Liggieri, L.; Sacca, L.; Clausse, D.; Ravera, F. *Colloids Surf., A* **2007**, *309*, 270.

surfactant concentration is high and the time scale of the rheological experiments is long. Whereas in Ostwald ripening the compression−expansion of surfactant layers is slow, film rupture occurs on very short time scales (milliseconds) and implies very rapid stretching of the layers during which bulk−surface exchange has no time to take place. The devices available to measure surface viscoelasticity at oil−water interfaces operate at low frequencies (below 1 Hz) and are unable to measure surface elasticities beyond this range. To be able to avoid the surface−bulk exchange, one can use very dilute solutions. The drawback is that the surfactant monolayers are less dense than those formed at the surface of the emulsion droplets, since the emulsions are made with concentrated surfactant solutions. In the present work, we found a compromise: we used nonionic surfactants with small micellar concentrations, allowing us to work close to the critical micellar concentration (cmc) where the monolayer is compact. We also used ionic surfactants for which electrostatic repulsion between the molecules and the interface slows down the exchanges.[8c] Finally, we used polymeric surfactants, which possess larger adsorption energies and are essentially irreversibly adsorbed.[11]

It is now recognized that the coalescence threshold is difficult to determine in emulsions unless the droplet size distribution is narrow enough because the threshold depends on the size: larger droplets coalesce faster with others than do small ones.[2] The threshold is also easier to define with concentrated emulsions. Above a droplet volume fraction of about 64% (random-close-packing volume fraction of spheres), the emulsions are viscoelastic and do not flow unless the yield stress is overcome.[12] The drops are no longer spherical and deform into polyhedra separated by thin liquid films. Coalescence is then easier to characterize because all liquid films have comparable thicknesses at a given time. In the case of concentrated emulsions, sedimentation or creaming have negligible effects, and the evolution due to Ostwald ripening and coalescence can be easily separated: in the early stages, the droplets are small and ripening is more efficient, whereas in later stages coalescence dominates. In this work, we used concentrated emulsions of oil volume fraction equal to 78%.

In earlier studies of concentrated monodisperse emulsions, it was demonstrated that the droplet diameter indeed first increases because of Ostwald ripening followed by coalescence.[13] The transition between the two regimes occurs at a critical droplet diameter. However, only a few emulsion types have been studied, and no correlation with interfacial viscoelasticity has been made to date.

In this article, we studied the time evolution of drop size in monodisperse concentrated emulsions. We used a broad range of systems: cationic, nonionic, and polymeric surfactants and alkanes of different chain lengths. We measured in parallel the surface response to expansion both at short times (using rapid expansions) and at longer times (using low-frequency sinusoidal expansions) in order to investigate possible correlations between surface elasticity and emulsion stability.

## II. Methods

In the present work, we used a pendent drop apparatus (IT Concept) to measure the dilatational elastic properties of oil/water interfaces. The drop is axysimetric, and its profile obtained from image analysis is fitted to the shape determined by the balance of gravity forces and capillary forces; this condition makes use of the Laplace equation for the pressure difference $\Delta p$ between the drop and the surrounding liquid

$$\Delta p = \gamma((1/R_1) + (1/R_2)) \quad (1)$$

where $R_1$ and $R_2$ are the two principal radii of curvature of the drop. We can measure in this way the surface tension $\gamma$ as a function of time.

A small drop is formed at the tip of a glass capillary inserted into a stainless steel needle by pushing the oil phase through a microsyringe driven by a motor-controlled device. The internal diameter of the glass capillary is 0.7 mm, and the wall thickness is 0.1 mm. The oil drop is surrounded by the aqueous solution of the surfactant. Prior to the experiment, the two phases were pre-equilibrated for at least 8 h. We performed a stress relaxation experiment in which, after reaching the equilibrium surface tension, the drop was first expanded and then kept at a constant size while the dynamic interfacial tension was monitored. The maximum interfacial tension right after the expansion was used to determine the interfacial elastic modulus

$$E = \frac{d\gamma}{d \ln(A/A_0)} \quad (2)$$

where $A$ is the area after expansion, and $A_0$ is the initial area of the drop.

During a fast enough expansion, there is no time for surfactant adsorption. The response to the expansion is purely elastic (in the absence of surface reorganization processes, very fast for surfactant molecules), and the elastic modulus is equal to

$$E_0 = -\frac{d\gamma}{d \ln \Gamma} \quad (3)$$

where $\Gamma$ is the surfactant concentration at the surface.

The elasticity was also measured at low frequencies by performing sinusoidal oscillations of the bubble volume. The measurement provides the real part $E_r$ and imaginary part $E_i$ of the elastic modulus: $E_i = \omega\kappa$, where $\omega = 2\pi\nu$, $\nu$ is the frequency, and $\kappa$ is the dilatational surface viscosity. When the surface−bulk exchanges are controlled by diffusion, the frequency variation of the dilational elasticity and viscosity are given by the Lucassen−van den Temple expressions[14]

$$E_r = E_0 \frac{1 + \Omega}{1 + 2\Omega + 2\Omega^2} \qquad E_i = \omega\kappa = E_0 \frac{\Omega}{1 + 2\Omega + 2\Omega^2} \quad (4)$$

where $E_0$ is the high-frequency elasticity, $\Omega = (\omega_0/\omega)^{1/2}$, and $\omega_0 = (D/2)\,(dC/d\Gamma)^2$, with $D$ being the surfactant diffusion coefficient and $C$ being its bulk concentration.

We also performed a number of emulsion studies. When Ostwald ripening dominates, theoretical models as well as experiments have revealed that the emulsions have a narrow size distribution in the asymptotic regime.[15,16]

(11) Rippner-Blomqvist, B.; Ridout, M. J.; Mackie, A. R.; Wärnheim, T.; Claesson, P. M.; Wilde, P. *Langmuir* **2004**, *20*, 10150. Hansen, F. K. *Langmuir* **2008**, *24*, 189.
(12) Mason, T. G.; Bibette, J.; Weitz, D. A. *Phys. Rev. Lett.* **1995**, *75*, 2051.
(13) Schmitt, V.; Leal-Calderon, F. *Europhys. Lett.* **2004**, *67*, 622. Schmitt, V.; Cattelet, C.; Leal-Calderon, F. *Langmuir* **2004**, *20*, 46.
(14) Lucassen, J. In *Anionic Surfactants: Physical Chemistry of Surfactant Action*; Lucassen-Reynders, E. H., Ed.; Marcel Dekker: New York, **1981**.
(15) Lifshitz, I. M.; Slyozov, V. V. *J. Phys. Chem. Solids* **1961**, *19*, 35.
(16) Kabalnov, A. S.; Makarov, A. V.; Pertzov, A. V.; Shchukin, E. D. *J. Colloid Interface Sci.* **1990**, *138*, 98.

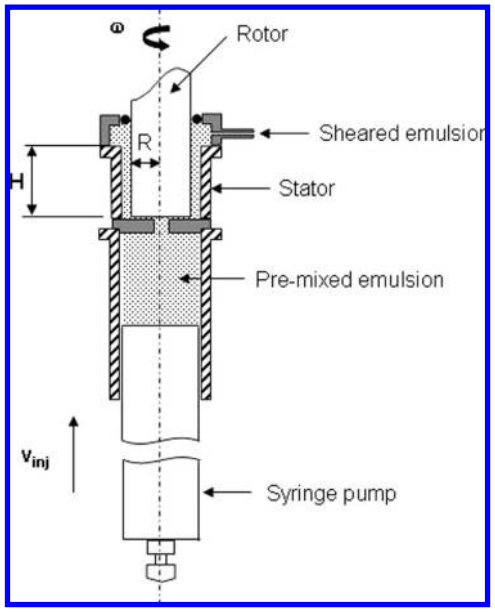


**Figure 1.** The premixed emulsion is inserted into the syringe and then pushed into the gap between the rotor and the stator. The final emulsion exits from the top of the mixer.[19]

Coalescence, on the contrary, leads to the rapid growth of polydispersity[17,18] until a layer of the dispersed phase forms (either at the top or the bottom of the container, depending on the relative oil and water densities).

A Couette-type mixer was used to fragment a premixed emulsion and to reduce the average drop diameter (Figure 1).[19] We obtained in this way concentrated emulsions with oil volume fractions of 78%. The droplet size distribution was measured at regular time intervals by using a Malvern Mastersizer laser granulometer. The collected scattering intensity as a function of the angle is transformed into a size distribution using Mie theory. The volume-averaged droplet size is defined as

$$D_v = (\sum_i N_i D_i^4)/(\sum_i N_i D_i^3) \quad (5)$$

with $N_i$ being the total number of droplets with diameter $D_i$. The polydispersity of the emulsion is characterized by $P$, defined as

$$P = 1/D_m((\sum_i N_i D_i^3 |D_m - D_i|)/\sum_i N_i D_i^3) \quad (6)$$

where $D_m$ is the median diameter (for which the volume fraction of droplets of size less than $D_m$ is equal to 50% of the total droplet volume fraction).

The regime of Ostwald ripening is characterized by a constant volume rate change $\Omega_3$ (diffusion-controlled ripening) or a constant surface rate change $\Omega_2$ (surface-controlled ripening)[4,13,19−21] depending on the origin of the dispersed-phase transfer mechanism

$$d(D_v)^\alpha/dt = \Omega_\alpha \quad (7)$$

where $\alpha = 3$ in the case of the volume-controlled process and $\alpha = 2$ if the process is surface-controlled. After rapid initial growth, the Ostwald ripening asymptotic regime is reached, where the distribution of droplet diameter is universal. This distribution is narrow; consequently, the emulsion is rather monodisperse.

When $D_v$ reaches a critical value $D^*$, Ostwald ripening and coalescence rates become equal: $(dD_v/dt)_{coal} = (dD_v/dt)_{Ost.rip}$. When $D_v > D^*$, coalescence becomes dominant.

## III. Chemicals

We studied a variety of surfactant systems at concentrations close or equal to the critical micellar concentration (cmc). These surfactants were of three types: ionic, nonionic, and polymeric. We have used two nonionic surfactants as received: *n*-dodecyl-$\beta$-maltoside ($C_{12}G_2$, cmc = $10^{-4}$ M) from Glyco and hexaethyleneglycol monododecyl ether ($C_{12}E_6$, cmc = $7 \times 10^{-5}$ M) from Sigma Aldrich. We also used *n*-alkyltrimethyl ammonium bromide cationic surfactants with different chain lengths from Sigma-Aldrich: DeTAB ($C_{10}$ chain), cmc = $5 \times 10^{-2}$ M; DTAB ($C_{12}$ chain), cmc = $1.4 \times 10^{-2}$ M; TTAB ($C_{14}$ chain), cmc = $4.4 \times 10^{-3}$ M; and CTAB ($C_{16}$ chain), cmc = $10^{-3}$ M. These surfactants were recrystallized three times in acetone, using traces of ethanol. We finally used two copolymers, Pluronic F-68 and Pluronic F-127, purchased from BASF: PE F/68, cmc = $9 \times 10^{-4}$ M; PE F/127, cmc = $5 \times 10^{-4}$ M. These surfactants are $(PEO)_x$-$(PPO)_y$-$(PEO)_x$ copolymers, with $x = 76$ and $y = 29$ for Pluronic F-68 and $x = 100$ and $y = 65$ for Pluronic F-127. They were washed thoroughly with hexane and dried under a vacuum pump. All of the aqueous solutions were prepared with Millipore water.

To clean the capillaries for the measurements of the rheological properties, we used an etching solution at the capillary tip (HF) while a constant flow of hexane was assured in order to avoid the penetration of the acid inside the capillary. The inner surface of the capillary was cleaned with hexamethyldisilazane ($C_6H_{19}Si_2N$) and washed with Millipore water.

We have used various alkanes as oils: heptane, octane, decane, and dodecane, purchased from Acros (>99%). For the preparation of the emulsions, we incorporated 2 wt % surfactant dissolved in 8 wt % water and 90 wt % oil. The two phases were premixed using gentle manual stirring, and coarse oil-in-water emulsions were obtained. These pre-emulsions were left to equilibrate for 1 night, and then subsequent fragmentation was performed in a Couette mixer (Ademtech) using a shear rate of 14 000 $s^{-1}$. The emulsions were then diluted to achieve an oil volume fraction of 78% and stored at room temperature. Small samples of the emulsion were taken at selected time intervals and diluted to perform the size measurement. The evolution of the emulsion drop size was monitored until a microscopic oil film appeared at the top of the sample.

## IV. Results and Discussion

**1. Interfacial Dilatational Rheology.** *a. Short-Time Response.* At the beginning of the experiment, an oil drop is formed. The surfactant begins to adsorb at the interface, and after a certain time, equilibrium interfacial tension is achieved. The drop is then suddenly expanded by introducing 1−4 $\mu$L of the oil phase into the drop. During the expansion from the initial area $A_0$ to the final area $A$, the concentration of the surface-active molecules at the oil/water

(17) Bibette, J.; Morse, D. C.; Witten, T. A.; Weitz, D. A. *Phys. Rev. Lett.* **1992**, *69*, 2439.
(18) Hasmy, A.; Paredes, R.; Sonneville-Aubrun, O.; Cabane, B.; Botet, R. *Phys. Rev. Lett.* **1999**, *82*, 3368.
(19) Mabille, C.; Schmitt, V.; Gorria, Ph.; Leal-Calderon, F.; Faye, V.; Deminiere, B.; Bibette, J. *Langmuir* **2000**, *16*, 422. Mabille, C.; Leal-Calderon, F.; Bibette, J.; Schmitt, V. *Europhys. Lett.* **2003**, *61*, 708.
(20) Wagner, C. *Z. Elektrochem.* **1961** *65*, 581.
(21) Durian, D. J.; Weitz, D. A.; Pine, D. J. *Phys. Rev. A 44*, R7902, **1991**

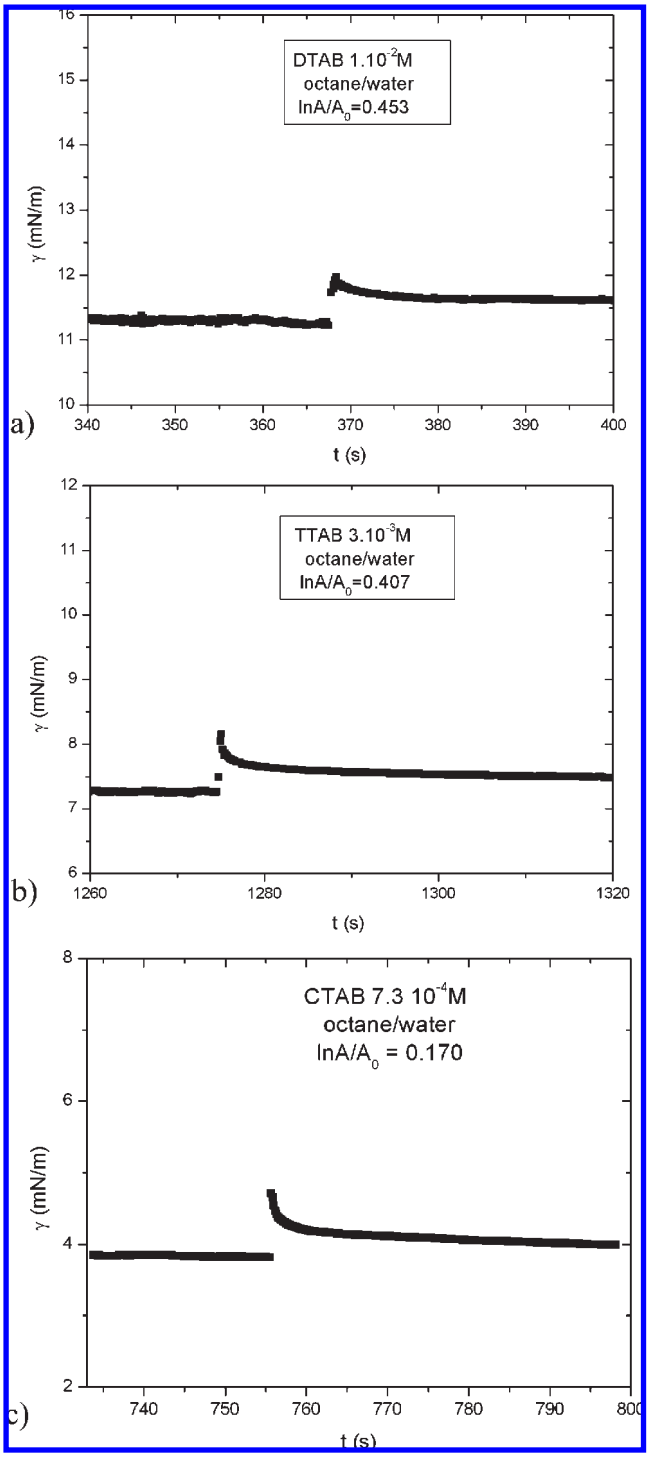


**Figure 2.** Equilibrium octane/water tension and interfacial tension variation with time after the area expansion for the cationic surfactants: (a) DTAB, (b) TTAB, and (c) CTAB.

interface drops, and the interfacial tension jumps to a higher value. Then the adsorption of molecules from the bulk to the interface takes place, and the tension decreases until it again reaches its equilibrium value (Figure 2). We performed at least seven jumps for each area augmentation to ensure the good reproducibility of our results. To evaluate the possible adsorption that took place during the expansion of the drop, we applied the procedure underlined in ref 22.

(22) Taylor, C. D.; Valkovska, D. S.; Bain, C. D. *Phys. Chem. Chem. Phys.* **2003**, *5*, 4885.

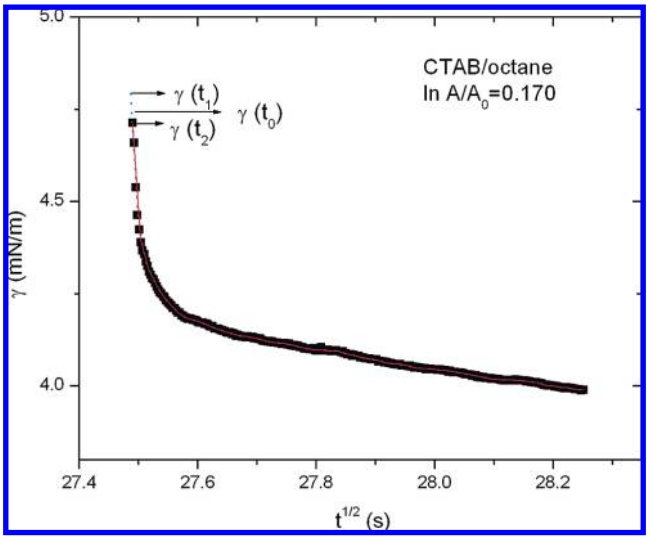


**Figure 3.** Relaxation curve for the CTAB/octane interface and extrapolation to $t_1$, the time at which the expansion begins. The difference in the surface tension at $t_1$ and $t_2$, the time at which the first measurement is made, gives the error bar of the measurement.

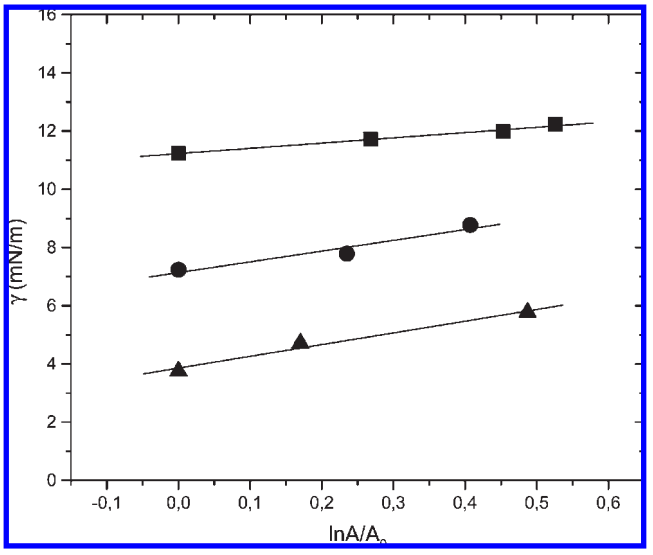


**Figure 4.** Interfacial tension measured after the augmentation of the surface area vs $\ln(A/A_0)$ plot and linear fits: (■) DTAB, (●) TTAB, and (▲) CTAB. The oil phase is octane.

We assume that adsorption is diffusion-controlled and that the time variation of the surface tension can be described by a polynomial function of $t^{1/2}$. We then use as the surface tension the average of the tension measured just after expansion ($t = t_2$) and the extrapolated tension at time $t_1$, where the expansion is started (Figure 3). We have taken as the error bar the difference $\gamma(t_1) - \gamma(t_2)$.

We measured in this way the surface tension as a function of the area expansion. Figure 4 shows the results for the cationic surfactants at the octane/water interface. For all of the systems studied, we obtain a linear relation with respect to the logarithm of the surface area ratio, showing that the response of the interface is linear (constant modulus $E$). The slope of these curves gives the elastic modulus according to eq 2. In the following text, we will consider that this modulus is high-frequency modulus $E_0$. The results are given in Table 1. The elastic modulus measured with DTAB was lower than with TTAB and CTAB, which have similar

**Table 1. Surface Properties**[a]

| surfactant/alkane | $C$ (M) | $\gamma$ (mN/m) | $E_0$ (mN/m) |
|---|---|---|---|
| DTAB/octane | $10^{-2}$ | 11.50 | $1.86 \pm 0.06$ |
| TTAB/octane | $3 \times 10^{-3}$ | 7.25 | $3.65 \pm 0.70$ |
| CTAB/octane | $7.3 \times 10^{-4}$ | 3.75 | $4.31 \pm 0.33$ |
| $C_{12}G_2$/octane | $10^{-4}$ | 4.57 | $17.15 \pm 0.39$ |
| $C_{12}E_6$/octane | $7 \times 10^{-5}$ | 23.20 | $6.37 \pm 0.58$ |
| TTAB/decane | $3 \times 10^{-3}$ | 7.76 | $3.38 \pm 0.17$ |
| TTAB/dodecane | $3 \times 10^{-3}$ | 7.78 | $3.03 \pm 0.06$ |
| $C_{12}G_2$/dodecane | $1 \times 10^{-4}$ | 5.12 | $17.67 \pm 0.50$ |
| PE F-68/heptane | $9 \times 10^{-4}$ | 13.59 | $11.92 \pm 0.73$ |
| PE F-127/heptane | $5 \times 10^{-4}$ | 5.39 | $11.23 \pm 0.87$ |

[a] Type of interface, surfactant concentration, interfacial tension, and high-frequency elasticity $E_0$. The expansion times for the measurement of $E_0$ are between 0.2 and 0.35 s.

values. We tried to measure the elastic modulus of the DeTAB water/octane interface, but the values detected were around zero. The measured interfacial tension was the highest for DTAB, followed by TTAB, and the lowest tension was obtained for CTAB. The values of the interfacial tension for all of the systems can also be found in Table 1.

To determine how the interfacial elasticity is influenced by the dispersed phase, we performed measurements using the same surfactant aqueous solution but oils with different chain lengths. We used TTAB and octane, decane, and dodecane. No significant change in the elastic moduli was found, although the tension is somewhat lower with octane (Table 1).

We performed the same kind of measurement with nonionic surfactant $C_{12}G_2$ and oils with different chain lengths. Again, no change in elasticity was seen between the octane/water and dodecane/water interfaces.

We have also studied the elastic properties of interfaces between octane and solutions of the two nonionic surfactants. The interfacial tension of the water/octane interface is much lower with $C_{12}G_2$ than with $C_{12}E_6$, but the elastic modulus with $C_{12}G_2$ is much higher than with $C_{12}E_6$ (Table 1).

We finally studied the two pluronics. The elastic moduli at the water/heptane interface were close, although the interfacial tension is significantly higher for PE F-68 (Table 1).

*b. Long-Time Response*. We also measured the low-frequency elasticity with the different surfactants. The results are displayed in Figure 5. One sees that the order changes significantly with respect to the high-frequency moduli: now the pluronic surfactants have the higher elastic moduli, and $C_{12}E_6$ moduli are vanishingly small at low frequencies. This is due in part to the bulk−surface exchanges. In the case of $C_{12}E_6$, these exchanges are important and faster than the time scale of the oscillatory compression used to obtain the data of Figure 5. During the drop oscillations, the surfactant molecules have enough time to dissolve in the bulk and to readsorb at the surface, resulting in little resistance to compression. Note that the time scale for this process is a diffusion time $\tau_D$ that strongly depends on concentration (eq 4). Larger moduli were obtained for $C_{12}G_2$ although the concentration used was larger; this is perhaps due to a different value of $dC/d\Gamma$ (eq 4) or to a possible adsorption−desorption barrier, in which case the frequency variation of the elastic moduli is no longer described by eq 4. This is certainly the case for pluronic surfactants that are polymeric species with high adsorption energies and are partially irreversibly adsorbed.[11] The case of cationic surfactants is more puzzling because the aqueous solutions are quite concentrated. In this case, however, there is an important

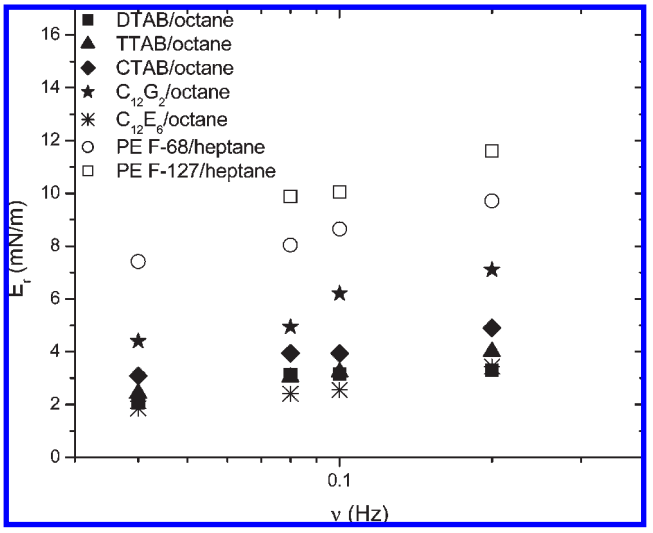


**Figure 5.** Frequency dependence of the real part of the elastic modulus for the different surfactants.

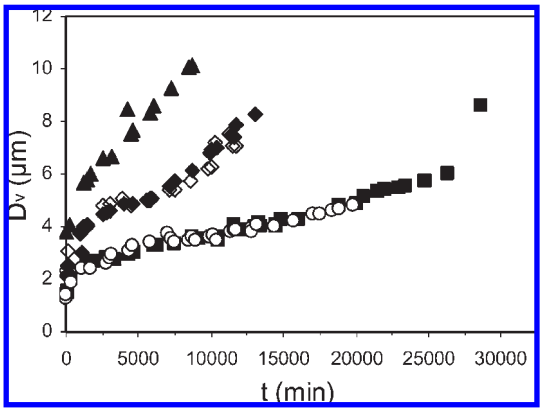


**Figure 6.** Evolution of the average diameter of the emulsion droplets as a function of time for (▲) DTAB, (♦) TTAB, (◇) CTAB, (■) $C_{12}G_2$, and (○) a 1:1 mixture of C12G2 and C12E6. The oil phase is octane.

adsorption barrier created by the charges of the surfactant molecules: in the absence of salt (charge screening), the elastic moduli are high, even at high concentrations.[8b,8c] The diffusion exchange is slowed down but still occurs: the lowest moduli are measured for the more concentrated systems (i.e., DTAB (Figure 5)) and increase from TTAB to CTAB.

**2. Emulsion Stability.** *a. Emulsions with Different Surfactants*. In Figure 6, volume-average drop diameter $D_v$ is plotted versus time for all of the emulsions made with octane and the short surfactants. The curves exhibit an inflection point at the critical diameter, $D^*$. At this point, Ostwald ripening and coalescence occur at the same rate. Before the critical diameter is reached, the rate-determining process governing the emulsion evolution is Ostwald ripening, and the polydispersity coefficient is around 20% (Figure 7). Once $D^*$ is reached, the rate-determining process is coalescence, and the polydispersity grows progressively. As can be seen in Figure 6, the lifetime of the emulsions made with the cationic surfactants is significantly shorter than the lifetime of the emulsions made with the nonionic ones. We studied the series DeTAB, DTAB, TTAB, and CTAB. The emulsions produced with DeTAB were extremely unstable. The oil phase and the water phase started to separate visibly in less than 8 h, and

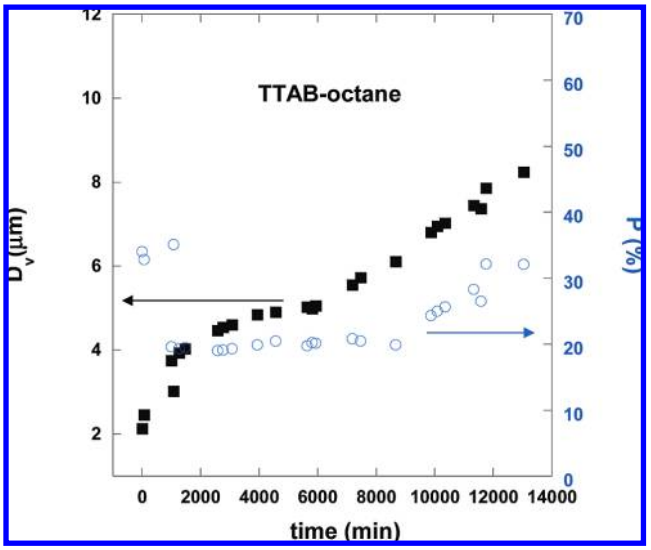


**Figure 7.** Time evolution of the droplet diameter (■) and polydispersity (○) for a TTAB/octane emulsion.

**Figure 8.** DeTAB emulsion in comparison to all the other octane systems: from left to right, DeTAB, DTAB, TTAB, CTAB, $C_{12}G_2$ + $C_{12}E_6$, $C_{12}G_2$; 8 h after production, the DeTAB/octane emulsion is phase-separated, and all of the other emulsions are stable.

we could not measure the coalescence frequency for this system (Figure 8). As we have mentioned earlier, we were not able to measure the elasticity at the oil/water interface for DeTAB because the values were zero within experimental error. We could perform more detailed studies with the other three cationic surfactants. The most unstable emulsion was that made with DTAB that has a lifetime of about 6 days. The TTAB and CTAB emulsions have similar evolutions and lifetimes (about 9 days). This is well correlated with surface elastic moduli, both at high and low frequencies: DTAB has the lowest modulus, and TTAB and CTAB showed almost the same values (Table 1).

We also investigated the emulsions made with nonionic surfactant $C_{12}G_2$, which were found to be very stable, whereas we could not produce emulsions using $C_{12}E_6$ only. This is well correlated with the low-frequency surface elastic moduli (and not with the high-frequency ones). The lifetime and evolution with the mixture and $C_{12}G_2$ were approximately the same.

The emulsions made with Pluronic surfactants were still more stable. In this case, we studied water−heptane

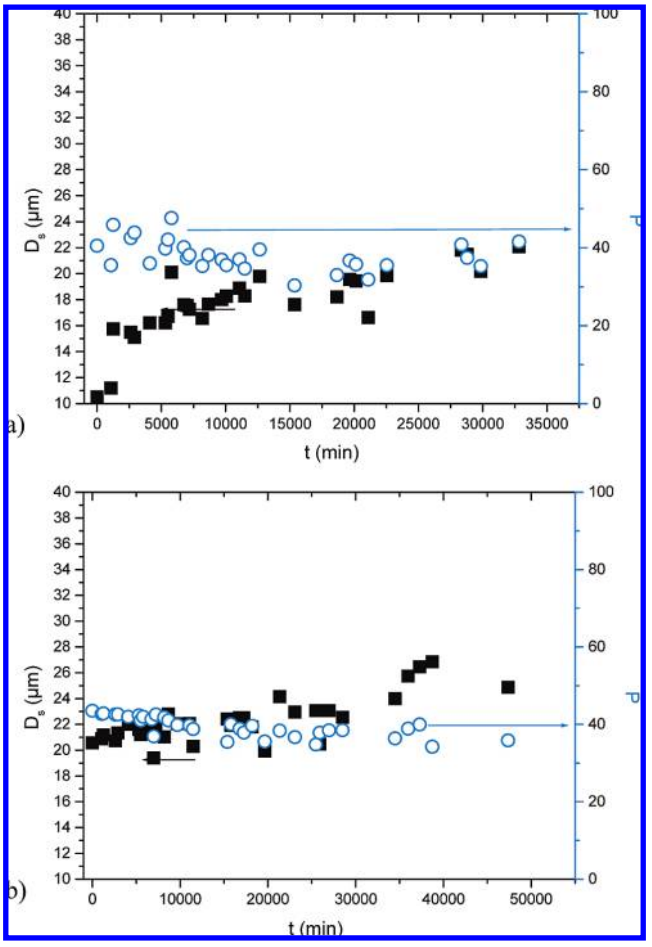


**Figure 9.** Pluronic PE F-68 (a) and Pluronic PE F-127 (b): evolution of the average diameter of the emulsion droplets as a function of time. The disperse phase is heptane.

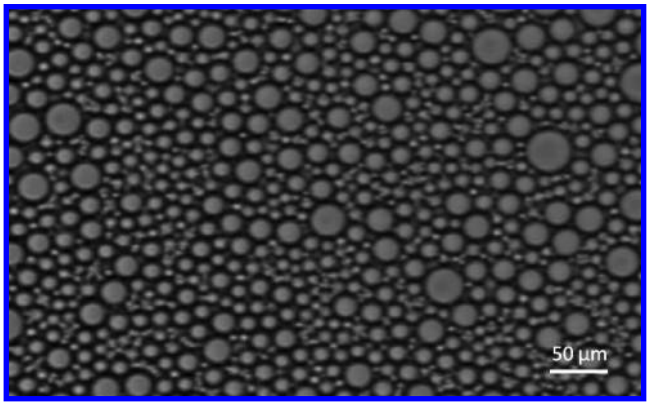


**Figure 10.** PE F-68/heptane emulsion right after its preparation. The average droplet diameter $D_v$ is on the order of 15 $\mu$m, and the polydispersity is about 50%.

emulsions in order to maximize Ostwald ripening, but even for this oil, little evolution of the drop size was seen (Figure 9). The average initial droplet diameter right after the fragmentation of the emulsion was much larger ($D_v$ = 15 $\mu$m) than for all of the other systems ($D_v$ = 2 $\mu$m) (Figure 10). We could not obtain a polydispersity of 20% with these systems although a polydispersity decrease with time was observed (from 45 to 32%) (Figure 9). This could be due, however, to the slow velocity of adsorption of these surfactants:[11] for the same energy input, there is likely more

coalescence during the emulsification process, resulting in a larger drop size and polydispersity. The same effect has been observed with foams.[23]

The emulsions stabilized by the polymeric surfactant remained stable for 1 month, after which $D_v$ did not appreciably increase: the emulsions were still in the transient Ostwald ripening regime, despite the high value of the average diameter. The high-frequency elastic moduli for the two pluronics were equal and about 11 mN/m (i.e., lower than for $C_{12}G_2$), which leads in principle to much less stable emulsions. However, the low-frequency elastic moduli are the highest among the different surfactants studied (Figure 5). Film rupture is in principle controlled by surface dilational elasticity, and because this rupture is very fast, it should be controlled by the high-frequency elasticity rather than by the low-frequency one. Ostwald ripening is mainly affected by the thickness of the films between bubbles and the solubility of gas in water. Van Vliet and co-workers[7] showed, however, that surface elasticity can appreciably slow the dissolution of bubbles in water, even stopping it when $E > \gamma/2$, as postulated earlier by Gibbs and Lucassen.[14] Because coarsening is slow, the elasticity to be considered here is the low-frequency elasticity. The bubble size evolves over time scales of thousands of minutes, hence the characteristic frequencies to be considered are on the order of $10^{-5}$ Hz or lower. If we assume that the trends shown in Figure 5 are conserved at these very lower frequencies, then we see that the rate of ripening follows the order of surface elastic moduli. This implies that the adsorption−desorption barriers responsible for the differences between the measured elasticities and the low values predicted by the Lucassen−van den Temple model are not overcome after long times. It was remarked that this is favored by interface vibrations.[8d] We can reasonably assume that the drop surfaces in the emulsions are protected from these vibrations and that the barriers remain effective for long times.

The highest moduli are measured for the pluronic surfactants that lead to the more stable emulsions. In this case, we even have $E > \gamma/2$, possibly explaining why ripening is very slow (Figure 9). However, the drops are about 10 times larger than with the short-chain surfactants, resulting in a coarsening rate ($dD_v/dt$) that is 100 times slower according to eq 7. Indeed, the experimental coarsening rate is on the order of $10^{-3}$ $\mu m^3/s$ (i.e., comparable to the rate for the short surfactants). This is the same as found earlier in more dilute emulsions.[24] Furthermore, the condition $E > \gamma/2$ applies provided the monolayer resists collapse: experiments on protein foams where the adsorption is also deemed irreversible and the compression moduli are high, show that these foams coarsen. This was recently explained by the existence of a collapse of the surface layers: above full protein coverage, the protein monolayer can continue to be compressed, forming multilayers.[7] The small bubbles can therefore continue to shrink, losing their spherical shape only when they are extremely small.[25] In this situation, coarsening can be avoided only if the surface layer thickness $d$ is large enough, above about $\langle D \rangle \gamma/E$.[7] A suppression of this type has been seen in mini-emulsions stabilized by thick polymer layers.[26]

(23) Georgieva, D.; Cagna, A.; Langevin, D. *Soft Matter*, DOI: 10.1039/B822568K.
(24) Kabalnov, A.; Weers, J.; Arlauskas, R.; Tarara, T. *Langmuir* **2006**, *22*, 1551.
(25) Dickinson, E.; Ettelaie, R.; Murray, B. S.; Du, Z. *J. Colloid Interface Sci.* **2002**, *252*, 202.
(26) Mun, S.; McClements, D. J. *Langmuir* **2006**, *22*, 1551.

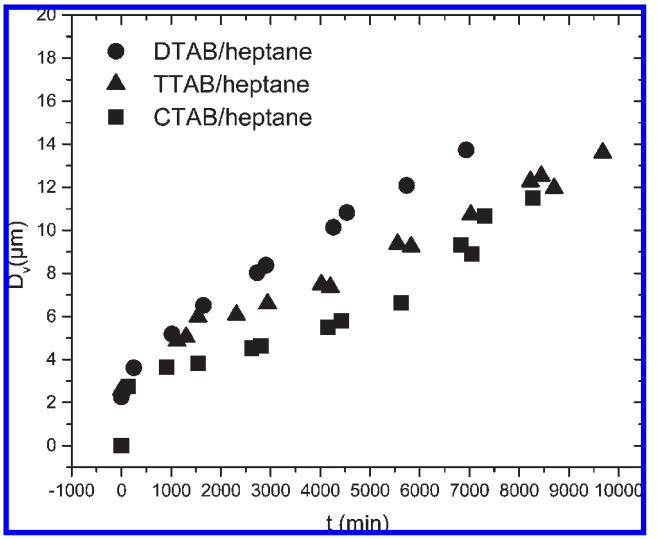


**Figure 11.** Evolution of the average diameter of the emulsion droplets as a function of time for (■) DTAB, (▲) TTAB, and (●) CTAB. The oil phase is heptane.

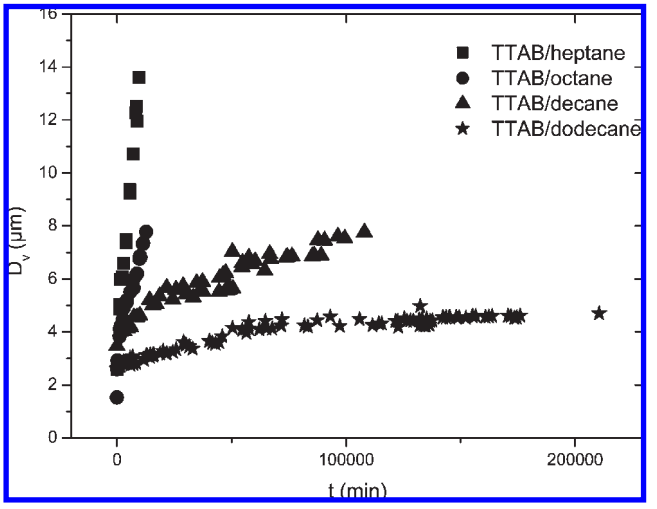


**Figure 12.** Evolution of the average droplet diameter with time for emulsions stabilized with TTAB but using different oils as the dispersed phase: (■) heptane, (●) octane, (▲) decane, and (★) dodecane.

We finally performed an additional measurement of the stability of DTAB, TTAB, and CTAB emulsions having heptane as a disperse phase (Figure 11). This study did not have the same accuracy as the octane study, but we saw the same tendencies in the behavior of the emulsions with respect to $D^*$ and $\Omega_\alpha$ as seen in the octane studies. The emulsions made with heptane were much less stable than those made with octane, which confirms the importance of Ostwald ripening in the emulsion destabilization

*b. Emulsions with Different Oils.* We also studied the influence of the oil chain length on the stability of the emulsions prepared with TTAB. The evolution of the droplet diameter as a function of time is presented in Figure 12. As was observed earlier by Schmitt and Leal-Calderon, the longer the chain of the oil, the more stable the emulsion.[13] Our results agree with this finding, which is not supported by the trend in surface elasticity: no change was seen for the different oils (Table 1). Here, however, the oil solubility has a strong effect on the Ostwald ripening process.

**Table 2. Critical Droplet Diameter $D^*$, Ostwald Ripening Rate $\Omega_3$, and Theoretical Rate $\Omega_{3\ theor}$**

| surfactant/alkane | $D^*$ ($\mu$m) | $\Omega_3$ ($\mu m^3$/s) | $\Omega_{3\ theor}$ ($\mu m^3$/s) | $\Omega_3/\Omega_{3\ theor}$ |
|---|---|---|---|---|
| DTAB/octane | 7.5 | $1.3 \times 10^{-3}$ | $5.17 \times 10^{-7}$ | |
| TTAB/octane | 5.5 | $3.3 \times 10^{-4}$ | $5.17 \times 10^{-7}$ | 640 |
| CTAB/octane | 5.5 | $3.1 \times 10^{-4}$ | $5.17 \times 10^{-7}$ | |
| $C_{12}G_2$/octane | 3.5 | $7.8 \times 10^{-5}$ | $5.17 \times 10^{-7}$ | |
| TTAB/decane | 6.7 | $1.1 \times 10^{-4}$ | $3.58 \times 10^{-8}$ | 3100 |
| TTAB/dodecane | 7 | $1.7 \times 10^{-6}$ | $2.56 \times 10^{-9}$ | 650 |
| TTAB/heptane | | $1.9 \times 10^{-3}$ | $2 \times 10^{-6}$ | 950 |

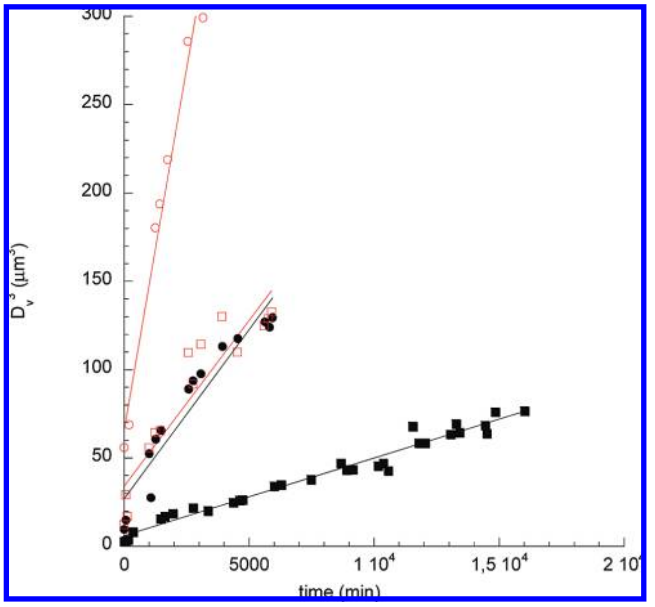


**Figure 13.** Third power of the mean diameter vs time ($D_v < D^*$) for the emulsions containing octane and (○) DTAB, (□) TTAB, (●) CTAB, and (■) $C_{12}G_2$. The lines are linear fits

*c. Main Parameters Determining the Stability of the Emulsions*. The numerical values of the critical diameter $D^*$ and the Otswald ripening rates were calculated with eq 7 with $\alpha = 2$ (surface-controlled process) and 3 (volume-controlled process). The accuracy of the data was not sufficient to discriminate between the two $\alpha$ values, and good fits were obtained in both cases. Figure 13 shows the $D_v^3$ versus time plots for the different emulsions containing octane.

The critical diameter $D^*$ in the case of octane as a disperse phase is not well defined for DTAB, which coarsens very rapidly. The emulsion droplets have almost the same critical diameter for TTAB and CTAB and a very similar evolution (Figure 7). The properties of the emulsions made with cationic surfactants change strongly when the chain length passes from 12 carbon atoms to 14, and then no significant evolution can be observed either in the emulsions or in the surface layers. This was also observed for foams.[27]

With $C_{12}G_2$, $D^*$ is even lower, although the emulsions are more stable. From Figure 6, it is clear, however, that the time needed to reach $D^*$ was much longer than for cationic surfactants. The rate of Ostwald ripening ($\Omega_3$) is decreasing as the emulsion becomes more stable. The lowest values were observed for the emulsion stabilized by $C_{12}G_2$ (apart from the pluronics). From the evolution curves, it can be seen that

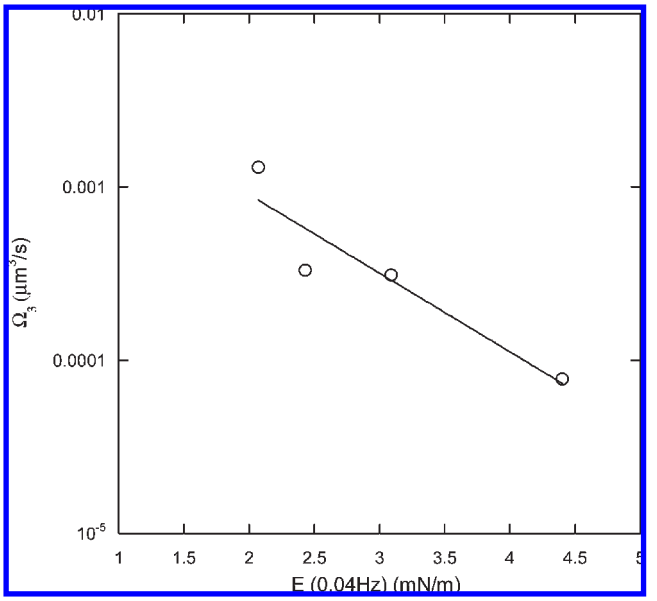


**Figure 14.** Experimental Ostwald ripening rate for octane emulsions vs surface elasticity measured at 0.04 Hz. The line is a fit with an exponential law.

the main process that governs the behavior of the emulsions is the Ostwald ripening. Very shortly after the transition to the coalescence regime, the oil film appears at the top of the sample, and we consider the emulsion to be destructed. That is why we think that the main parameter that we should regard as a measure of the emulsion stability is the rate of Ostwald ripening. This confirms the relevance of the low-frequency elasticity. Figure 14 illustrates the dependence of the Ostwald ripening rate with the low-frequency elasticity: in the small parameter window probed here, this dependence is quite significant. (The line is a fit with exponential variation.)

The theoretical ripening rate calculated for dilute emulsions is

$$\Omega_{3\ theor} = \frac{64\gamma D_{oil} S V_m}{9RT} \quad (8)$$

where $D_{oil}$ is the diffusion coefficient of oil molecules in water, $S$ is the oil solubility in water, $V_m$ is the molar oil volume, $R$ is the gas constant, and $T$ is the absolute temperature.[4,15] The calculated and measured rates are given in Table 2. It is not surprising to find much faster measured rates because the drops are very close in the emulsions studied and oil transfer is much easier. Similar discrepancies were found earlier by other authors.[13,28] When comparing the results for TTAB and the different oils, the rather constant ratio of theoretical and measured values confirms that the differences in ripening rates are due to differences in oil solubility in water ($\gamma$ varies much less, see Table 1). For the emulsions made with octane, the measured Ostwald ripening rate is clearly not proportional to surface tension as predicted by eq 8 (Tables 1 and 2); as discussed above, it correlates much better with the low-frequency elasticity (Figure 14). The theoretical description of the Ostwald ripening process in the regime studied here where the emulsions droplets are slightly distorted into polyhedric shapes with different numbers of faces (of different concavity and

(27) Bergeron, V. *Langmuir* **1997**, *13*, 3474.

(28) Weiss, J.; Herrmann, N.; McClements, D. J. *Langmuir* **1999**, *15*, 6552.

hence different local ripening rates),[29] where liquid transfer occurs across the films between flattened drops and in interstices between drops, and where surface elasticity limits the ripening is clearly too complex to be achieved. Numerical simulations might be able to bring solutions to this difficult problem in the future.

## V. Conclusions

In this work, we have measured the surface elasticities of oil drops immersed in surfactant aqueous solutions by submitting them to rapid expansion and monitoring the surface tension evolution. Experiments were performed at the interfaces between octane and aqueous solutions of $C_nTAB$ ($n$ = 12, 14, 16), $C_{12}G_2$, $C_{12}E_6$, and two pluronics (PE F-68 and PE F-127). We have also measured the surface elasticities of TTAB with other oils, decane and dodecane, and $C_{12}G_2$ with dodecane. In the case of the water/octane interface, the elastic modulus $E_0$ measured for DTAB was lower than that for TTAB and CTAB, which have similar values. The elastic moduli for the nonionic surfactants are significantly larger, with the modulus for $C_{12}G_2$ being about 3 times larger than for $C_{12}E_6$ and 50% larger than for the pluronics. There is no significant change in the elastic modulus when the oil is changed.

Strikingly, the elastic moduli measured at low frequencies fall in different orders: the larger moduli are seen for the pluronics, followed by $C_{12}G_2$ and the cationic series, with the values for $C_{12}E_6$ being the smallest. This is likely due to different relaxation processes specific to the different surfactants: $C_{12}E_6$ is believed to exchange freely between the surface and bulk during periodic compression, whereas adsorption/desorption barriers (electrostatic in the case of the cationic surfactants) slow down the exchange process.

The emulsion studies showed that the emulsions produced with DTAB/octane were less stable than the TTAB and CTAB/octane emulsions that evolved very similarly. Still more stable emulsions were obtained with $C_{12}G_2$, whereas those made with $C_{12}E_6$ were so unstable that they could not be produced. These results do not follow the order of the high-frequency elastic modulus, which is supposed to control coalescence. In turn, they are well correlated with the low-frequency moduli, which are expected to control the Ostwald ripening process. This is consistent with the time evolution of the drop diameter, clearly dominated by the ripening process. Little time evolution was observed in the case of emulsions made with the pluronics: in this case, the initial drop size is large, and although the ripening rate is similar to that of the other surfactants, the process is slow.

It should be noted that because the coalescence probability increases with drop size the evolution seen here might be different than the evolution of emulsions prepared with larger drop sizes. Further work is planned to explore this regime. The results obtained so far demonstrate the great importance of surface elasticity in emulsion stability.

**Acknowledgment.** D.G. is grateful for the financial support of the European Commission under the 6th Framework Program (contract no. MRTN-CT-2004-512331-Project SOCON). We gratefully thank C. Stubenrauch for numerous stimulating discussions concerning the measurement of surface elasticity.

(29) Lambert, J.; Cantat, I.; Delannay, R.; Mokso, R.; Cloetens, P.; Glazier, J. A.; Graner, F. *Phys. Rev. Lett.* **2007**, *99*, 058304.